Global Mineralogical and Aqueous Mars History Derived from OMEGA/Mars Express Data

Jean-Pierre Bibring,[1] Yves Langevin,[1] John F. Mustard,[2] François Poulet,[1] Raymond Arvidson,[3] Aline Gendrin,[1,2] Brigitte Gondet,[1] Nicolas Mangold,[4] P. Pinet,[5] F. Forget,[6] the OMEGA team[7]

Global mineralogical mapping of Mars by the Observatoire pour la Mineralogie, l'Eau, les Glaces et l'Activité (OMEGA) instrument on the European Space Agency's Mars Express spacecraft provides new information on Mars' geological and climatic history. Phyllosilicates formed by aqueous alteration very early in the planet's history (the "phyllocian" era) are found in the oldest terrains; sulfates were formed in a second era (the "theiikian" era) in an acidic environment. Beginning about 3.5 billion years ago, the last era (the "siderikian") is dominated by the formation of anhydrous ferric oxides in a slow superficial weathering, without liquid water playing a major role across the planet.

The earliest observations of Mars by spacecraft showed that water had caused substantial erosion of the surface, including extensive channeling and associated transport and deposition of material (*1*). However, fundamental questions remain. Was water-driven activity on its surface transient or persistent, the latter being a prerequisite to sustain habitable surface environments? When and where did that activity take place, and when did it end? Mineralogical thermal infrared mapping from the Mars Global Surveyor Thermal Emission Spectrometer (MGS TES) suggests that Mars must have been cold and dry over most of its history (*2*–*4*). In a few locations, however, gray hematite was detected and was interpreted to result from aqueous processes (*2*, *5*, *6*). In Terra Meridiani, the Mars Exploration Rover (MER) Opportunity revealed that sulfates formed in the presence of water and that the hematite found by TES consists of concretions weathered from the sulfate deposits (*7*). New data from the Mars Express OMEGA (Observatoire pour la Minéralogie, l'Eau, les Glaces et l'Activité) instrument (*8*, *9*), in combination with local ground information from the MERs, provide extensive information on the aqueous history of Mars and the mineralogical evolution of its crust.

Surface mineralogy. After 1 martian year of operation in orbit around Mars, OMEGA has mapped 90% of the surface at a spatial sampling of 1.5 to 5 km and ~5% of the surface at a sampling of <0.5 km; on each pixel, the spectrum from 0.35 to 5.1 μm is acquired. OMEGA spectral data allow the identification of a variety of mafic and altered minerals, typically at a volume concentration of 5% or greater. For hydrated minerals and a few others, the sensitivity is even higher.

Fe-bearing pyroxene is the most widely distributed mineral detected by OMEGA (*10*) (Fig. 1) and previous instruments (*2*–*4*); both high-calcium pyroxene (HCP) and low-calcium pyroxene (LCP) have been identified by OMEGA through their spectral features from 0.7 to 2.5 μm. LCP-rich areas are observed within the ancient Noachian crust. HCP-rich areas are mapped in more recent lava flows. Olivine is also found either in these pyroxene-rich terrains or in localized areas in which olivine dominates, mostly within crater floors and rims, and proximal to large impact basins (*11*). The identification and distribution of these mafic minerals are consistent with and extend previous observations using thermal infrared measurements (*12*). On a global scale, both pyroxene and olivine are still present at the surface in the older terrains, including within sand dunes. However, much of the younger surface, particularly within the large lowlands of the northern hemisphere (Fig. 1), does not exhibit the spectral signatures of these Fe-bearing mafic minerals: The exposed original constituents have been heavily altered or covered by heavily altered dust. This alteration of the martian surface material has not occurred merely through physical weathering, such as through the grinding of bedrock into sand and dust. Surface texture from high-resolution imaging [by the MGS Mars Orbiter Camera (MOC) and Mars Express High-Resolution Stereo Camera (HRSC)], thermal inertia from infrared (IR) behavior [from the MGS TES and the Mars Odyssey Mission Thermal Emission Imaging System (Odyssey THEMIS)], and pyroxene content from near-IR hyperspectral imagery (from OMEGA) are not systematically coupled: Terrains of similar pyroxene content are found as both bedrock and dunes, and terrains with similar soil properties are found with different pyroxene content. Laboratory data and remote sensing of the Moon (*13*) demonstrate that mafic regolith grains can exhibit their diagnostic spectral signatures after extended exposure that includes meteoritic impact (forming high concentrations of glasses) and solar wind irradiation. In the wide areas of Mars with no mafic signatures, the surface material is thus made of grains and rocks that have been chemically altered, as mobile dust and/or in situ–processed bedrock.

OMEGA data contribute to the identification of these altered phases and to the search for the potential role that water played in that alteration: OMEGA allows discrimination among gas, frost, ice, water absorbed, and water bound in hydrated minerals. High-albedo regions distributed across Mars show specific absorption features from 0.4 to 1.3 μm attributed to Fe^{3+} (Fig. 1) and are thus oxidized. These results extend previous observations made from Earth (*14*), and from the rovers on Mars (*15*). The OMEGA spectra of these oxidized minerals lack the absorption signatures of hydrated minerals (Fig. 2A): The minerals are not hydrated nor do they require the presence of liquid water to form. The alternative interpretation that they result from a dehydration of hydroxides (such as goethite or palagonite) is not validated by the OMEGA detection of a variety of hydrated silicates (clay minerals) and sulfates in old terrains. Liquid water is not responsible for Mars being red.

The grain size of these anhydrous ferric oxides that dominate in the bright areas is likely

[1]Institut d'Astrophysique Spatiale (IAS), Bâtiment 121, 91405 Orsay Campus, France. [2]Department of Geological Sciences, Brown University, Providence, RI 02912, USA. [3]Department of Earth and Planetary Sciences, Washington University, St. Louis, MO 63130, USA. [4]Interactions et Dynamique des Environnement de Surface (IDES), Bâtiment 509, 91405 Orsay Campus, France. [5]Observatoire Midi-Pyrénées, Toulouse, France. [6]Laboratoire de Météorologie Dynamique (LMD), Université Paris 6, Paris, France. [7]The OMEGA co-investigator team: Michel Berthé,[1] Jean-Pierre Bibring,[1] Aline Gendrin,[1] Cécile Gomez,[1] Brigitte Gondet,[1] Denis Jouglet,[1] François Poulet,[1] Alain Soufflot,[1] Mathieu Vincendon,[1] Michel Combes,[2] Pierre Drossart,[2] Thérèse Encrenaz,[2] Thierry Fouchet,[2] Riccardo Merchiorri,[2] GianCarlo Belluci,[3] Francesca Altieri,[3] Vittorio Formisano,[3] Fabricio Capaccioni,[4] Pricilla Cerroni,[4] Angioletta Coradini,[4] Sergio Fonti,[5] Oleg Korablev,[6] Volodia Kottsov,[6] Nikolai Ignatiev,[6] Vassili Moroz,[6] Dimitri Titov,[6] Ludmilla Zasova,[6] Damien Loiseau,[7] Nicolas Mangold,[7] Patrick Pinet,[8] Sylvain Douté,[9] Bernard Schmitt,[9] Christophe Sotin,[10] Ernst Hauber,[11] Harald Hoffmann,[11] Ralf Jaumann,[11] Uwe Keller,[12] Ray Arvidson,[13] John F. Mustard,[14] Tom Duxbury,[15] François Forget,[16] G. Neukum,[17] [Affiliations for the OMEGA team: [1]IAS, Orsay Campus, France. [2]Laboratoire d'Etudes Spatiales et d'Instrumentation en Astrophysique, Observatoire de Paris, Meudon, France. [3]Istituto di Fisica della Spazio Interplanetario–Istituto Nazionale di Astrofisica (IFSI-INAF), Rome, Italy. [4]IAS-INAF, Rome, Italy. [5]University of Lecce, Italy. [6]Institut Komichiski Issledovanie, Moscow, Russia. [7]IDES, Orsay Campus, France. [8]Observatoire Midi-Pyrénées, Toulouse, France. [9]Laboratoire de Planétologie, Grenoble, France. [10]Departement de Planétologie, Université de Nantes, France. [11]Deutsches Zentrum für Luft- und Raumfahrt, Berlin, Germany. [12]Max-Planck-Institut für Sonnensystemforschung, Lindau, Germany. [13]Department of Earth and Planetary Sciences, Washington University, St. Louis, MO, USA. [14]Department of Geological Sciences, Brown University, Providence, RI, USA. [15]Jet Propulsion Laboratory, Pasadena, CA, USA. [16]LMD, Université Paris 6, Paris, France. [17]Freie Universität, Berlin, Germany.]

very small, and they might be nanocrystalline red hematite α-Fe_2O_3 or possibly maghemite γ-Fe_2O_3. Such small particles would be easily transported, stick on most grains, and account for the magnetic properties of the soil measured by the MERs (*16*). Ferric oxides are also detected in localized areas with a variety of albedo (such as within Terra Meridiani, Valles Marineris, or Aram Chaos).

Two types of hydrated minerals have been identified from OMEGA data: phyllosilicates (*10*, *17*) (Fig. 2B) and sulfates (*10*, *18*–*20*) (Fig. 2C), but in only a few locations (*17*) (Fig. 3). Carbonate-rich areas have not been found by OMEGA, although a low concentration of carbonate is interpreted from TES data on martian dust (*21*), and carbonates are recognized in martian meteorites (*22*).

From their near-IR (0.8 to 2.6 μm) spectra, we infer that most of the phyllosilicate minerals are Fe-rich (such as chamosite and nontronite), although Al-rich phyllosilicates (such as montmorillonite) are locally dominant (*17*). These clay minerals are found in a variety of light-toned outcrops and scarps, primarily in rocks and soils north of the Hesperian-aged Syrtis Major volcanic plateau, Nili Fossae, and the Marwth Vallis regions. In all these regions, phyllosilicates are mapped associated with ancient Noachian-aged surfaces. For example, in Nili Fossae, thin Noachian-aged but unaltered mafic units rest directly on phyllosilicate-bearing outcrops. Information from the Mars Express HRSC, the MGS MOC, and the Odyssey THEMIS images clearly indicates that the phyllosilicates are in rocks buried by more recent deposits; the hydrated silicate-bearing bedrock has been exposed through erosion. The surface material of Noachian terrains, which are identified as being heavily cratered, does not necessarily all date from the Noachian times. Rocks of Noachian age are exposed in spots because of impact, faulting, or erosion.

In the Syrtis Major and Nili Fossae regions, phyllosilicate-rich rocks are detected in both ancient craters and material recently excavated from ancient terrains beneath a later volcanic cover. These relations demonstrate that these impacts did not dehydrate the minerals. In contrast, no hydrated minerals are detected in the lobate craters (thought to form by impact into volatile-rich substrates) within the lava flows from Nili Patera, which embay the ancient terrains (*10*). This relation suggests that mineralization of hydrated minerals occurred before the emplacement of the Hesperian-aged lavas from Nili Patera and that these lavas are essentially water-free. In the Marwth Vallis region (Fig. 4), hydrated minerals are not found in the channel nor in its opening but rather on the surrounding plateau and its eroded flanks. Thus, water associated with the formation of the channel did not lead to phyllosilicate formation, although this outflow was sufficient to produce severe erosion, including exposing the ancient clay-rich minerals. So far, none of the major and minor outflow channels or the valley networks show evidence of hydrated minerals.

Sulfates, including Mg sulfates (such as kieserite) and Ca sulfates (such as gypsum), constitute the second major class of hydrated minerals mapped by OMEGA and detected by the NASA rovers (*7*). OMEGA has shown that the sulfate-rich areas are not restricted to the gray hematite-rich regions detected by the MGS TES (*2*, *5*, *6*). We have detected three principal types of hydrated sulfate deposits: layered deposits within Valles Marineris, extended deposits exposed from beneath younger units as in Terra Meridiani, and the dark dunes of the northern polar cap (*10*, *18*–*20*).

Sequential mineral formation. Environments conducive to clay mineral formation may have existed at or near the surface or in the deeper subsurface. Surface or near-surface conditions would not require high-temperature conditions (hydrothermal, for example). Surface formation of these clay minerals would indicate a long-lasting wet episode, with large surface aqueous reservoirs and alkaline water resulting from this chemical alteration, occurring during the Noachian.

Clay minerals could also have been formed primarily in the subsurface, by one of the three following processes: hydrothermal activity (*23*); cratering, supplying subsurface water (liquid and/or ice) to the impacted minerals (*24*); or during the cooling of the mantle, if not thoroughly depleted of volatile compounds. These deep scenarios would not require a warm Mars to have existed over extended time scales, and they could have taken place even if Mars never sustained a dense atmosphere. In addition, the formation of clay minerals could have continued at greater depths long after conditions at the surface became unfavorable.

Sulfate mineral formation requires substantial quantities of water to account for the broad distribution of minerals seen by OMEGA. Because sulfate precipitation requires water to evaporate, it is essentially a surface process. For at

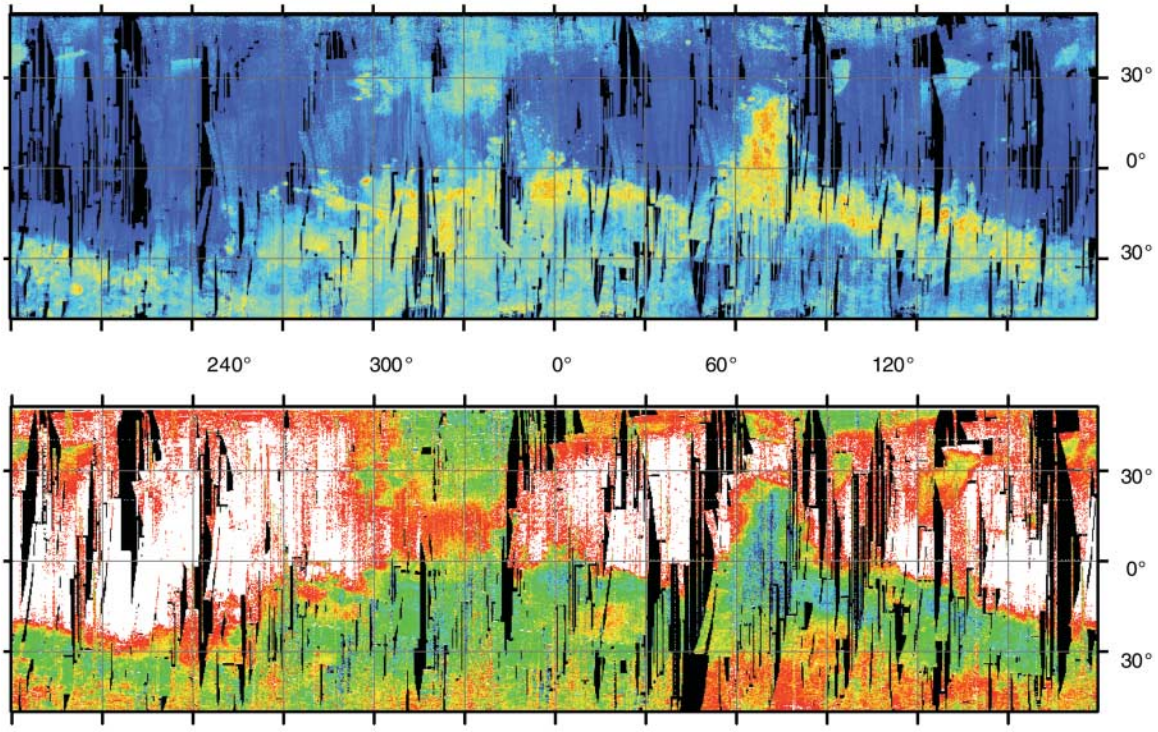

Fig. 1. Global maps of pyroxene (**top**) and anhydrous nanophase ferric oxides (**bottom**), exhibiting the anticorrelation between surface mafics and altered minerals (in the form of ferric oxides). The cratered crust with large pyroxene content (top, yellow to red) is not covered with altered minerals (bottom, blue to green). Conversely, the large areas with no mafics (top, blue) correspond to the higher concentration of ferric oxides (bottom, red to white).

least some of the sulfates identified, an acidic environment is also required. On this basis, we infer that extensive sulfate minerals formed from the late Noachian to the Hesperian, after the surface formation of phyllosilicates, which indicates a substantial change in the global aqueous chemistry of Mars. In addition to their younger age, the sulfate-rich deposits observed by OMEGA extend over a large region. Their size requires a large source of sulfur that we propose is a direct consequence of the extensive outpourings of lavas and associated degassing that primarily formed Tharsis Plateau, as well as the northern plains (in a lunar mare–like process) and Hesperian ridged plains (*25*, *26*). This period of peak volcanism was probably accompanied by a huge release of volatiles, including sulfur and water. This sulfur would have been rapidly oxidized in the atmosphere to form H_2SO_4, which then precipitated on the surface. Surface water would result from a combination of outgassing, hydrothermal activity, the rise of the water table, and massive outflows as Valles Marineris opened, over extended periods of time. All the ingredients were in place for extensive sulfate deposition, either by means of acidic alteration or by weathering of both mafic minerals and, locally, their phyllosilicate alteration products.

Although carbonate minerals have been invoked as a possible reservoir for an early thick CO_2 atmosphere in contact with persistent liquid water (*27*), none have been detected above the OMEGA sensitivity limit of 4% in volume abundance. This result indicates that (i) the era during which surface liquid water remained stable did not last long enough to enable large amounts of CO_2 from the primordial denser atmosphere to be transformed into carbonates; or (ii) clay minerals were formed by impact or subsurface hydrothermal processes rather than by slow surface alteration within liquid water, leaving most of the primordial CO_2 in the atmosphere; or (iii) carbonates have been eliminated from the near surface by acidic weathering or decomposition; or (iv) Mars never sustained a dense CO_2-rich atmosphere. OMEGA data indicate no present major CO_2 reservoirs other than in the atmosphere or the thin CO_2 permanent ice cap over the southern pole (*10*, *28*). This cap is only a thin veneer, typically some meters deep, thus accounting for a small fraction (~10% at most) of the present atmospheric CO_2. On board the NASA Mars Reconnaissance Orbiter, the Compact Reconnaissance Imaging Spectrometers for Mars will perform hyperspectral near-IR mapping with 10 times better spatial resolution than OMEGA: The potential detection of carbonates in association with either phyllosilicates or rocks exposed by impacts should provide constraints against these different possibilities.

After the formation of phyllosilicates and sulfates, the third alteration era began and has continued up to the present, in which liquid water did not play an important role. This is evidenced by the lack of hydration of the ferric oxides, in contrast with the detection of hydrated phyllosilicates and sulfates. Liquid water was probably present during transient and local events (such as the release of volatiles by impacts or the melting of ice deposits), but these episodes were too short to leave a substantial mark on the surface composition. Thus, these transient water events are not responsible for the global alteration, which has mostly been caused by surface oxidation and the production of nanophase ferric oxide, without hydration (Fig. 1). Formation of this alteration product could result from gas/solid reactions (such as atmospheric weathering), mainly through peroxide reactivity or perhaps by frost/rock interactions. This type of alteration probably occurred throughout the three eras. However, it became dominant only in the latter era, when the other sources, which led to the formation of phyllosilicates then sulfates, faded out. The low current H_2O_2 content (*29*), if representative of the entire third era, makes this a slow process, affecting only the superficial layer. This hypothesis is supported by observations of a thin alteration rind on basaltic rocks observed by the Spirit rover at the Gusev landing site (*7*, *30*, *31*). This rind is at most a few millimeters thick and the underlying rock is unaltered. It is also consistent with the low albedo of the material within the trenches made by the MERs in the PanCam images (*31*), indicating that the covering soil and the alteration layer together are a few millimeters thick at most. This slow atmospheric alteration process also accounts for the presence of unaltered mafic minerals in areas either recently brought to the surface (by impact or erosion) or consisting of ancient high-altitude terranes, which have been exposed to much-reduced atmospheric peroxide activity. The presence of nanophase ferric oxide materials across broad regions such as Tharsis, Arabia, and Hellas indicates that these alteration products have been

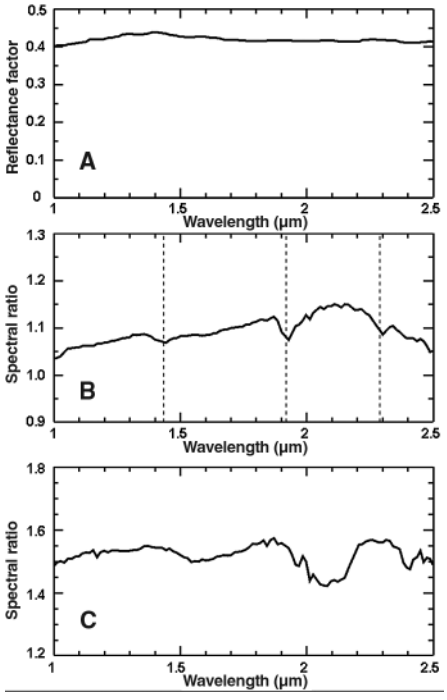

Fig. 2. OMEGA spectra of (**A**) a bright anhydrous soil, rich in nanophase ferric oxides; (**B**) a typical Fe-rich phyllosilicate area; and (**C**) a Mg-sulfate deposit.

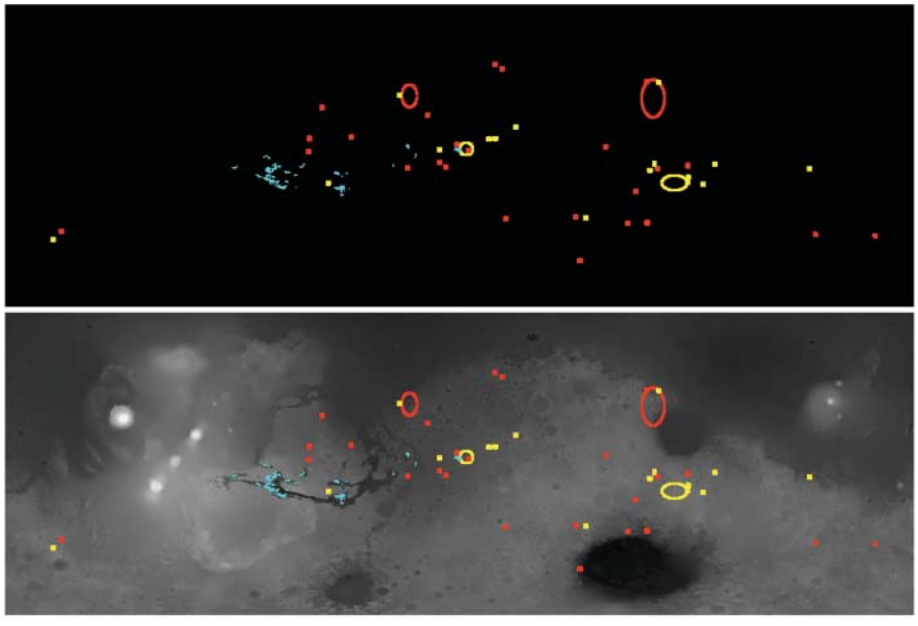

Fig. 3. Global map of hydrated minerals (**top**) plotted over a MGS Mars Orbiter Laser Altimeter (MOLA) altitude reference map (**bottom**). Red, phyllosilicates; blue, sulfates; yellow, other hydrated minerals, with no marked feature (such as being driven by metal-OH vibration) enabling the identification.

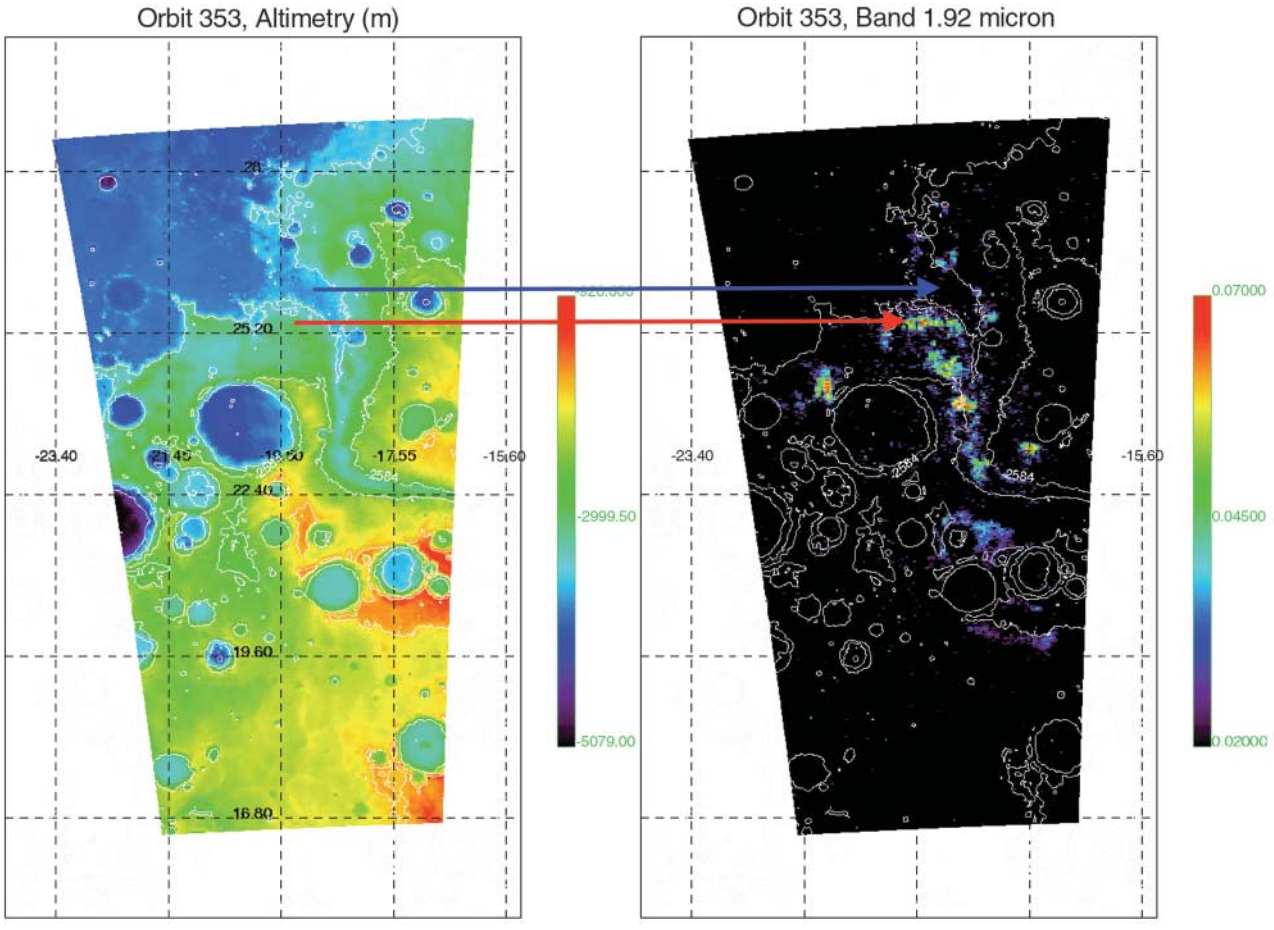

Fig. 4. Magnification of one area of the global map of hydrated minerals (Fig. 3), mapping the hydrated sites in the Marwth Vallis region, with its context in a MGS MOLA altimetry map. Hydrated minerals are not found in the channel (blue arrow) but in the eroded flanks and the cratered plateau (red arrow).

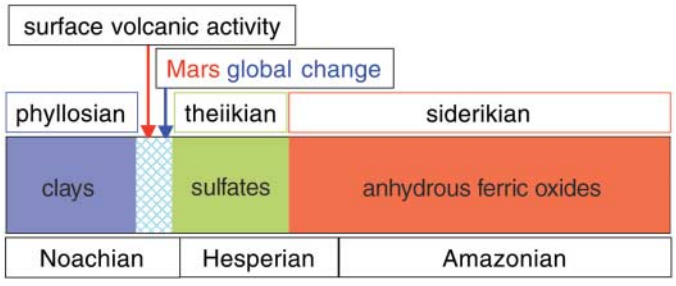

Fig. 5. Sketch of the alteration history of Mars, with phyllosilicates formed first, then sulfates, then anhydrous ferric oxides.

redistributed by atmospheric and aeolian processes across the planet.

Derived Mars history. Our analysis of OMEGA mineralogical assignments in the context of the geologic history of Mars indicates three sequential eras characterized by the surface alteration products (Fig. 5): (i) a nonacidic aqueous alteration, traced by phyllosilicates (the "phyllosian" era); (ii) an acidic aqueous alteration, traced by sulfates (the "theiikian" era); and (iii) an atmospheric aqueous-free alteration, traced by ferric oxides (the "siderikian" era)

The transition between the first two eras occurred early in time and during a critical episode of Mars global climate change from an alkaline, possibly moist, environment to an acidic environment. This change was driven by the extensive outgassing of volatiles, including sulfur, coupled to the volcanic activity that modeled Mars' surface. If phyllosilicates had formed in the subsurface, the Mars environment might have always been tenuous, cold, and dry, except for transient episodes.

If instead phyllosilicates formed at or close to the surface, this would require the Mars early atmosphere to be dense. The global change to an acidic environment would then have been coupled to a rapid drop in atmospheric pressure. A number of processes can be invoked to account for it. The heavy bombardment of Mars, given its low mass, could have resulted in an efficient escape of its early atmosphere (*32*). The global change could also have been triggered by a rapid drop of the internal dynamo and its resulting magnetic shield, favoring efficient atmospheric sputtering (*32*, *33*).

The era during which Mars might have been most likely to have hosted habitable conditions is the first one, indicated by the presence of phyllosilicates. If indeed living organisms formed, these clay minerals could be the sites in which this biochemical development took place (*34*). The low level of the further surface alteration, in perennial cold and dry conditions, under a tenuous atmosphere, could have preserved most of the record of biological molecules, structures, or other diagnostic features in clay-rich surface or subsurface rocks. These areas of high habitability potential offer exciting targets for future in situ exploration.

References and Notes

1. M. H. Carr, *Water on Mars* (Oxford Univ. Press, New York, 1996).
2. P. R. Christensen *et al.*, *J. Geophys. Res.* **106**, 23 (2001).
3. P. R. Christensen *et al.*, *J. Geophys. Res.* **106**, 823 (2001).
4. P. R. Christensen *et al.*, *J. Geophys. Res.* **106**, 871 (2001).
5. P. R. Christensen, R. V. Morris, M. D. Lane, J. L. Bandfield, M. C. Malin, *J. Geophys. Res.* **106**, 873 (2001).
6. P. R. Christensen, R. V. Morris, M. D. Lane, J. L. Bandfield, M. C. Malin, *J. Geophys. Res.* **106**, 885 (2001).

7. S. W. Squyres *et al.*, *Science* **306**, 1709 (2004).
8. J.-P. Bibring *et al.*, *Eur. Space Agency Spec. Publ.* **1240**, 37 (2004).
9. A. Chicarro, P. Martin, R. Trautner, *Eur. Space Agency Spec. Publ.* **1240**, 3 (2004).
10. J.-P. Bibring *et al.*, *Science* **307**, 1576 (2005).
11. J. Mustard *et al.*, *Science* **307**, 1594 (2005).
12. J. L. Bandfield, *J. Geophys. Res.* **107**, 5092 (2002).
13. C. M. Pieters, in *Remote Geochemical Analysis: Elemental and Mineralogic Composition*, C. M. Pieters, P. A. J. Englert, Eds. (Cambridge Univ. Press, New York, 1993), pp. 309–340.
14. P. Pinet, S. Chevrel, *J. Geophys. Res.* **95**, 14435 (1990).
15. J. F. Bell III *et al.*, *J. Geophys. Res.* **105**, 1721 (2000).
16. P. Bertelsen *et al.*, *Science* **305**, 827 (2004).
17. F. Poulet *et al.*, *Nature* **438**, 623 (2005).
18. A. Gendrin *et al.*, *Science* **307**, 1587 (2005).
19. Y. Langevin, F. Poulet, J.-P. Bibring, B. Gondet, *Science* **307**, 1584 (2005).
20. R. Arvidson *et al.*, *Science* **307**, 1591 (2005).
21. J. L. Bandfield, T. D. Glotch, P. R. Christensen, *Science* **301**, 1084 (2003).
22. J. C. Bridges *et al.*, *Space Sci. Rev.* **96**, 365 (2001).
23. L. L. Griffith, E. L. Shock, *J. Geophys. Res.* **102**, 9135 (1997).
24. H. E. Newson, *Icarus* **44**, 207 (1980).
25. X. Phillips *et al.*, *Science* **291**, 2587 (2001).
26. S. C. Solomon *et al.*, *Science* **307**, 1214 (2005).
27. R. Kahn, *Icarus* **62**, 175 (1985).
28. J.-P. Bibring *et al.*, *Nature* **428**, 627 (2004).
29. T. Encrenaz *et al.*, *Icarus* **170**, 424 (2004).
30. R. V. Morris *et al.*, *Science* **305**, 833 (2004).
31. See plates in (*35*).
32. E. Chassefière, F. Leblanc, *Planet. Space Sci.* **52**, 1039 (2004).
33. B. M. Jakovsky, R. J. Phillips, *Nature* **412**, 237 (2001).
34. J. D. Bernal, *The Physical Basis of Life* (Routledge & Kegan Paul, London, 1951).
35. J. F. Bell III *et al.*, *Science* **305**, 800 (2004).
36. The OMEGA instrument was developed with the support of the Centre National d'Etudes Spatiales (CNES), Agenzia Spatiale Italiana (ASI), and Russian Space Agency. The scientific activity is funded by national space and research agencies and universities in France, Italy, Russia, Germany, and the United States. We are very grateful to all of the European Space Agency (ESA) teams who, together with industry, enable this mission. Public OMEGA data are accessible on the ESA Planetary Science Archive Web site. This paper benefited from very valuable comments from S. Murchie.

15 November 2005; accepted 20 March 2006
10.1126/science.1122659

Structure and Receptor Specificity of the Hemagglutinin from an H5N1 Influenza Virus

James Stevens,[1]* Ola Blixt,[1,2] Terrence M. Tumpey,[4] Jeffery K. Taubenberger,[5] James C. Paulson,[1,2] Ian A. Wilson[1,3]*

The hemagglutinin (HA) structure at 2.9 angstrom resolution, from a highly pathogenic Vietnamese H5N1 influenza virus, is more related to the 1918 and other human H1 HAs than to a 1997 duck H5 HA. Glycan microarray analysis of this Viet04 HA reveals an avian α2-3 sialic acid receptor binding preference. Introduction of mutations that can convert H1 serotype HAs to human α2-6 receptor specificity only enhanced or reduced affinity for avian-type receptors. However, mutations that can convert avian H2 and H3 HAs to human receptor specificity, when inserted onto the Viet04 H5 HA framework, permitted binding to a natural human α2-6 glycan, which suggests a path for this H5N1 virus to gain a foothold in the human population.

The H5N1 avian influenza virus, commonly called "bird flu," is a highly contagious and deadly pathogen in poultry. Since late 2003, H5N1 has reached epizootic levels in domestic fowl in a number of Asian countries, including China, Vietnam, Thailand, Korea, Indonesia, Japan, and Cambodia, and has now spread to wild bird populations. More recently, the H5N1 virus has spread to infect bird populations across much of Europe and into Africa. However, its spread to the human population has so far been limited, with only 191 documented severe infections, but with a high mortality accounting for 108 deaths in Indonesia, Vietnam, Thailand, Cambodia, China, Iraq, Turkey, Azerbaijan, and Egypt [as of 4 April 2006, see the World Health Organization Web site (*1*)]. Of these, evidence suggests direct bird-to-human transmission, although indirect transmission, perhaps through contaminated water supplies, cannot be ruled out.

Of the three influenza pandemics of the last century, the 1957 (H2N2) and 1968 (H3N2) pandemic viruses were avian-human reassortments in which three and two of the eight avian gene segments, respectively, were reassorted into an already circulating, human-adapted virus (*2*, *3*). The origin of the genes of the 1918 influenza virus (H1N1), which killed about 50 million people worldwide (*4*), is unknown. The extinct pandemic virus from 1918 has recently been reconstructed in the laboratory and was found to be highly virulent in mice and chicken embryos (*5*, *6*). With continued outbreaks of the H5N1 virus in poultry and wild birds, further human cases are likely, and the potential for the emergence of a human-adapted H5 virus, either by reassortment or mutation, is a threat to public health worldwide.

Hemagglutinin (HA), the principal antigen on the viral surface, is the primary target for neutralizing antibodies and is responsible for viral binding to host receptors, enabling entry into the host cell through endocytosis and subsequent membrane fusion. As such, the HA is an important target for both drug and vaccine development. Although 16 avian and mammalian serotypes of HA are known, only three (H1, H2, and H3) have become adapted to the human population. HA is a homotrimer; each monomer is synthesized as a single polypeptide (HA0) that is cleaved by host proteases into two subunits (HA1 and HA2). HA binds to receptors containing glycans with terminal sialic acids, where their precise linkage determines species preference. A switch in receptor specificity from sialic acids connected to galactose in α2-3 linkages (avian) to α2-6 linkages (human) is a major obstacle for influenza A viruses to cross the species barrier and to adapt to a new host (*7*, *8*). On H3 and H1 HA frameworks, as few as two amino acid mutations can switch human and avian receptor specificity.

Of the H5N1 viral isolates studied to date, A/Vietnam/1203/2004 (Viet04) is among the most pathogenic in mammalian models, such as ferrets and mice (*9*, *10*). This virus was originally isolated from a 10-year-old Vietnamese boy who died from bird flu. Because of the importance of HA in viral pathogenesis and host response to viral infection, we cloned and expressed the ectodomain (HA0) of its HA gene (fig. S1) in a baculovirus expression system, using the same strategy that led to the crystal structure of the 1918 influenza virus HA0 (*11*, *12*). Viet04 HA0 was cleaved during protein production into its activated form (HA1/HA2) and was crystallized at pH 6.55 (*13*). Its structure was determined by molecular replacement (MR) to 2.95 Å resolution (table S1) (*14*). In addition, we have investigated the potential of this H5 HA to acquire human receptor specificity by introducing mutations known to effect such a specificity switch on H1 and H3 frameworks.

Structural overview. The overall fold of the Viet04 HA trimer (Fig. 1, A and B) is very similar to other published HAs, as expected, with a globular head containing the receptor binding domain (RBD) and vestigial esterase domain, and a membrane proximal domain with its distinctive, central α-helical stalk and HA1/HA2 cleavage site (essential for viral pathogenicity). Although Viet04 HA and the only other avian H5 HA structure, Sing97 [A/Duck/Singapore/3/1997; Protein Data Bank (PDB) entry 1jsm (*15*)], are closely related in sequence (HA1, 90%; HA2, 98%), the best molecular replacement (MR) solutions were sur-

[1]Department of Molecular Biology, [2]Glycan Array Synthesis Core-D, Consortium for Functional Glycomics, [3]Skaggs Institute for Chemical Biology, The Scripps Research Institute, 10550 North Torrey Pines Road, La Jolla, CA 92037, USA. [4]Influenza Branch, Division of Viral and Rickettsial Diseases, Centers for Disease Control and Prevention, Atlanta, GA 30333, USA. [5]Department of Molecular Pathology, Armed Forces Institute of Pathology, Rockville, MD 20306, USA.

*To whom correspondence should be addressed. E-mail: wilson@scripps.edu (I.A.W.) and jstevens@scripps.edu (J.S.)